Numerical modeling on sediment capture in catch basins

Haoming Yang, David Z. Zhu and Lin Li

ABSTRACT

Catch basins are designed to convey surface runoff into sewer systems. They are also found to be effective in retaining sediments. A number of factors can influence catch basin sediment capture efficiency, such as sediment size distribution, flow hydraulics and catch basin design. To better understand the influence of these factors, numerical simulations using the Eulerian-Lagrangian method were conducted to provide insights into flow fields and to predict sediment capture rates. The numerical model was validated using previous experimental measurements of flow field and sediment capture rates for sediment sizes larger than 0.25 mm. The influence of catch basin designs, including the bottom sump and inflow arrangements, was also studied, and an equation was developed for predicting the capture rate.

Key words | capture efficiency, catch basin, computational fluid dynamics, numerical modeling, particle tracking, sediment

Haoming Yang
David Z. Zhu
Department of Civil Engineering,
Zhejiang University,
Hangzhou 310027,
China

Lin Li (corresponding author)
College of Water Conservancy and Civil Engineering,
Xinjiang Agricultural University,
Urumqi 830052,
China
E-mail: *lilin_xjau@163.com*

Haoming Yang
David Z. Zhu
Lin Li
Department of Civil and Environmental Engineering,
University of Alberta,
Edmonton, AB,
Canada, T6G 2W2

INTRODUCTION

Catch basins are designed to receive surface runoff and they can also play a vital role in retaining sediments in storm sewer systems (Aronson *et al.* 1983). Sediments may reduce the capacity of sewers and adhere pollutants. Therefore, efforts have been devoted to investigating the efficiency of sediment capture in catch basins. Previous studies (Howard *et al.* 2011; Tang *et al.* 2016) indicate that a number of factors can affect capture efficiency. Typical sediments found in catch basins are non-cohesive, with a specific gravity of around 2.40 to 2.80 (Chebbo *et al.* 1990; Butler *et al.* 1992; Clegg *et al.* 1992). Sediment size is also a key variable in determining the settling ability. According to several previous studies (Almedeij *et al.* 2010; City of Calgary 2011; Bong *et al.* 2014), the size of bed load sediments in catch basins is usually larger than 0.2 mm. In addition, flow hydraulics and structures of catch basins also impact on capture efficiency.

Several laboratory experiments (Lager *et al.* 1977; Aronson *et al.* 1983; Howard *et al.* 2011, 2012; Tang *et al.* 2016) have been conducted to study sediment removal ability in various catch basins. Wilson *et al.* (2009) and Howard *et al.* (2011) developed equations for estimating the capture rate under different scenarios. However, existing experiments are still limited, and the effects of some factors are still unclear as detailed measurements in catch basins are difficult to obtain (e.g. particle movements and flow field). Also, the test range in experimental studies is often restricted (e.g. the maximum flow rate) due to limitations in laboratory capacities.

Compared to laboratory studies, numerical simulation can be a less expensive and more efficient alternative to gain insights into detailed fluid fields and particle dynamics. Faram & Harwood (2000) commented that once validated, computational fluid dynamics (CFD) is a tool with reliability and efficiency to help design storm sewer systems. Currently, there are two common approaches to studying sand/water two-phase flows, namely, the Eulerian-Eulerian method and the Eulerian-Lagrangian method. The Eulerian-Eulerian method is proven to be successful in predicting the mixture of two or more different phases (Sha *et al.* 2001; Kee & Tan 2002; Wang *et al.* 2006; Virdung & Rasmuson 2007; Azimi *et al.* 2012). However, the Eulerian-Lagrangian method is found to be more suitable in predicting particle capture behaviors (Wörner 2003). For instance, Faram & Harwood (2002) used the Reynolds Stress turbulence model to obtain the flow field and the Lagrangian particle tracking method to predict particle trajectories in

doi: 10.2166/wst.2018.009

storm water treatment chambers. Thinglas & Kaushal (2008) tested FLUENT software (Fluent Manual 2005) with the renormalisation group (RNG) k-ε model along with the discrete particle model to simulate particle trapping in an invert trap. Chrigui (2005) focused on the interactions between solid particles and flow coupling with particle tracking procedure. Mohsin & Kaushal (2016) applied a three-dimensional simulation with volume of fluid (VOF) model to predict solids trap efficiency in an invert trap fitted in an open channel.

In this study, a water-air-solid three-phase numerical model was built to simulate the sediment capture process in catch basins. The objectives of this study are: (1) to predict the capture rate of the catch basin under extended flow conditions, (2) to investigate the flow field and the particle transport process, (3) to evaluate the impact of the bottom sump and the inflow arrangement on the capture rate, and (4) to develop an equation for predicting the capture rate under different scenarios.

NUMERICAL MODEL

In this study, the commercial software ANSYS CFX 15.0 (ANSYS CFX 2013) was used to solve the governing equations. The RNG k-ε model was chosen for the turbulence closure of water flow, and the Lagrangian tracking method was used to study the sediment movement. In addition, VOF model was used to predict the water surface level. The study was based on steady-state simulations and the governing equation (Reynolds-averaged Navier-Stokes equation) can be expressed as followed:

$$u_i \frac{\partial(\rho u_i)}{\partial x_i} = -\frac{\partial p}{\partial x_i} + \rho g_i + \mu \frac{\partial^2 u_i}{\partial x_j \partial x_j} - \frac{\partial \rho\left(\overline{u_i' u_j'}\right)}{\partial x_j} \quad (1)$$

where u is the mean velocity and p is the pressure term, i and j are equal to 1, 2, or 3, representing three directions in the Cartesian coordinate system, g is the gravitation acceleration and ρ is the density. The term $-\rho(\overline{u_i' u_j'})$ is the Reynolds Stress.

In this study, the particle volume loading is very low (less than 10^{-6}). Thus while the motion of particles are influenced by the surrounding flow, the particles are assumed to have negligible influence on the flow field (Chrigui 2005). Therefore, a one-way coupling model is chosen in the simulation, which has a significant advantage in saving computation resources as the Eulerian velocity field can be computed independently of particle tracking. For the discrete-phase tracking method, the particle trajectories are calculated by integrating the force balance on the particles. The equation for force balance in x-direction in the Cartesian coordinates can be written as:

$$\frac{du_p}{dt} = F_D(u_w - u_p) + \frac{G_x(\rho_p - \rho_w)}{\rho_p} + F_x \quad (2)$$

where u_w and u_p represent the velocity of water and particles, respectively, and ρ_w and ρ_p are the density of fluid and particles, respectively. Forces acting on the simulated particles include several components: $F_D(u_w - u_p)$ is the drag force per unit particle mass, G_x is the gravity term, and F_x is the additional acceleration term which can be important under certain circumstances. For instance, 'virtual mass' force is considered due to the fact that the particle has to accelerate some of the surrounding fluid, leading to an additional drag force. At the same time, the turbulent dispersion force arises due to pressure gradient in the fluid. Generally, the drag force is the dominating factor. In this study, the drag force of the spherical particles was acquired by the Schiller and Naumann model (Wörner 2003).

MODEL SETUP AND VALIDATION

In the numerical modeling, the configuration and settings were set to match the laboratory settings of Tang *et al.* (2016), see Figure 1(a). The catch basin has a square shape of 0.9 m with a height of 1.3 m. A sump with a depth of 0.5 m can be covered by a false bottom. The inlet of the catch basin is simplified as a circular pipe with a diameter of 150 mm. This inlet simplification will likely produce a lower sediment capture rate (i.e. more conservative) due to the stronger turbulence the inflow jet produces compared to the field cases. The rest of the top is open, allowing air to move in and out. The outlet pipe is located at the side of the bottom with a diameter of 250 mm, and has a slope of 1/200 to help drain the water. The bottom of the outlet pipe is considered as the datum.

In the experiments of Tang *et al.* (2016), solids with a specific gravity of 2.65 were added after the flow became steady-state. The top of the catch basin was set as an open boundary condition with atmospheric pressure, except the

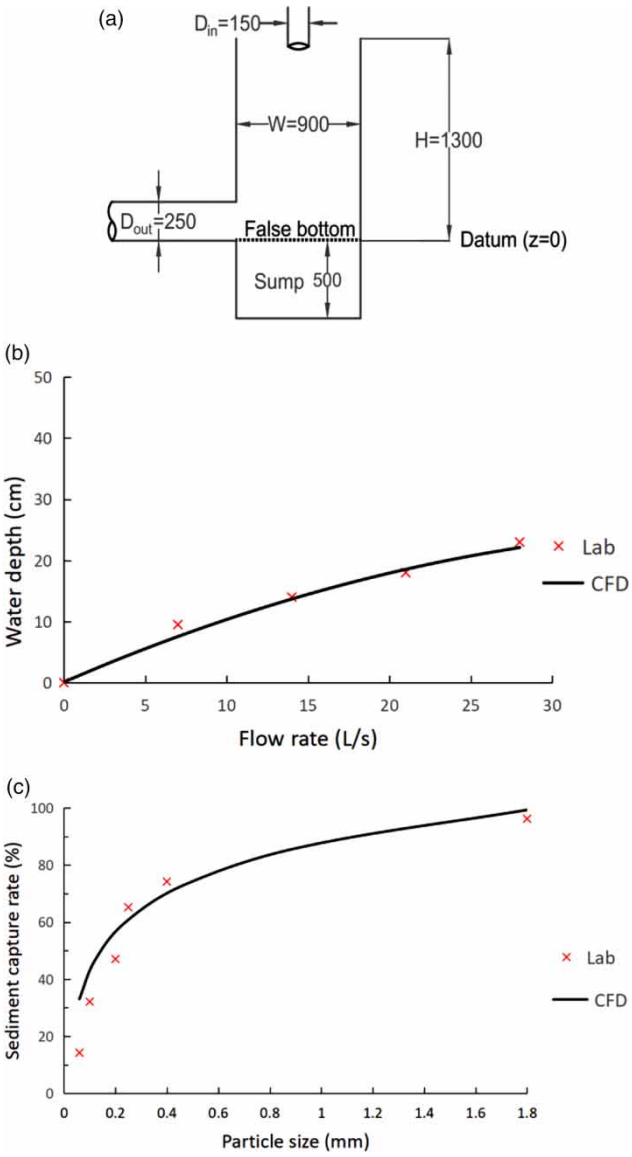

Figure 1 | (a) Side view of the study catch basin of Tang *et al.* (2016); all dimensions are in mm). Comparisons of the simulations and the measurements of: (b) water depth and (c) sediment capture rates at a flow rate of 28 L/s.

inlet pipe which was set as the inlet boundary with a specified flow rate. The pressure outlet condition was set at the end of the outlet pipe. In the modeling, 100,000 particles of uniform size were injected at the inlet boundary with zero slip velocity. The particle-wall interaction involves complex process and can be affected by multiple factors (e.g. wall material, wall roughness, impact angle and velocity). In this study, a reflecting wall boundary coupled with the virtual rough wall Sommerfeld-Frank model (Niño & García 1998) was used. In the reflecting boundary condition, the parallel and the perpendicular restitution coefficients were used to describe the decay rate of particle velocity when hitting a wall and both were set as 0.75.

Unstructured meshes were generated by Ansys-Mesh, and four groups of meshes with different resolutions were built. The water depth and the sediment capture rate were chosen as the objectives to test the mesh independence. By comparing the results with different mesh resolutions, it was found that the results show little difference compared to the results with a finer mesh size when the node number attained about one million. Therefore, the group of meshes with 1,030,191 nodes and 1,951,324 elements was used in this study to ensure both computational efficiency and accuracy. The convergence targets were set as 10^{-4} for momentum and mass residual. At the same time, mass imbalance was set as 0.01. Furthermore, under the same conditions, the simulated results including water depth as well as sediment capture rate were compared with the experimental results (Tang *et al.* 2016) as shown in Figure 1(b) and 1(c). The water depth rises with the increase of flow discharge and the CFD simulations show good agreement with the measurements. For the capture rate, the numerical predictions show little difference compared with the laboratory results when particle size is larger than 0.25 mm. However, when the particle is smaller than 0.2 mm, the prediction tends to overestimate the capture rate, and the error becomes greater for smaller particles.

Due to the absence of flow field measurement in the experiment of Tang *et al.* (2016), results from the laboratory study of Howard *et al.* (2011) were used to validate the flow field modeling. In the experiment, flow measurements were obtained using a three-dimensional acoustic Doppler velocimeter. The experimental setup is shown in Figure 2(a): the sump is circular with a diameter of 1.2 m and a depth of 1.2 m; the inlet and outlet pipes are the same size. The maximum discharge in the experiment was 170 L/s, and the simulations were compared with the experimental results. The velocity components in the sump in vertical direction (V_z) are normalized by the mean velocity in the pipe (V_{jet}), and the normalized velocity components along the depth are shown in Figure 2(b).

As is shown, the simulated maximum velocity agrees well with the measurement. Also, the simulated results predict well the variation of the velocity along the depth under different flow rates. At a flow rate of 127 L/s, the normalized vertical velocity components always show negative values, while with a larger flow rate of 170 L/s, the velocity tends to show values with a variation tendency from negative to positive.

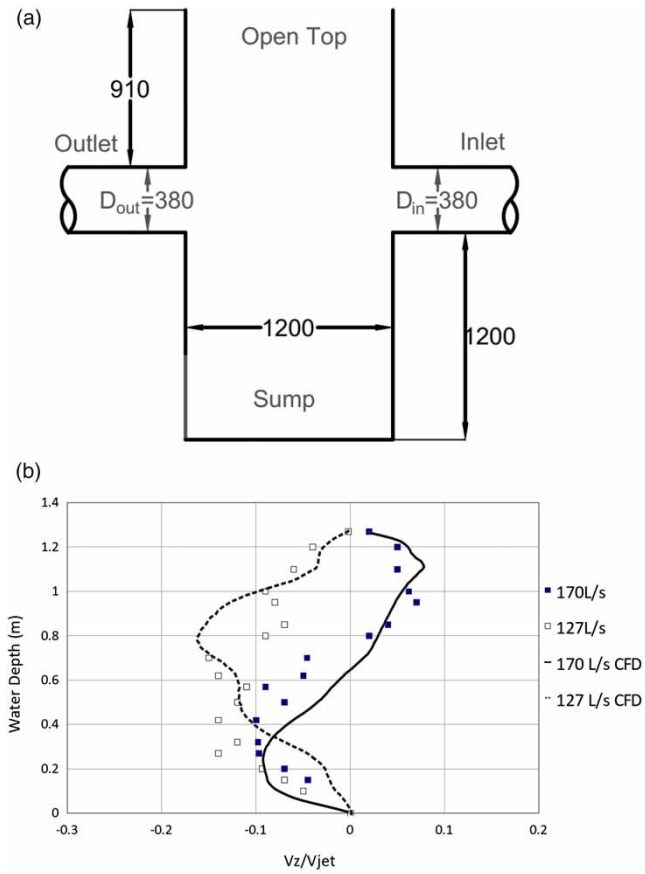

Figure 2 | (a) Side view of the experimental setup of Howard *et al.* (2011); all dimensions are in mm. (b) Distribution of the normalized vertical velocity at two flow rates. Measurements were taken at 0.4 m upstream of the outlet in the center plane.

RESULTS AND DISCUSSION

One of the advantages of numerical modeling is its ability to extrapolate the study range without limitations in laboratory studies. In the experiment of Tang *et al.* (2016), the maximum flow rate tested was limited to around 30 L/s due to the experimental conditions; therefore, simulations were carried out to investigate the sediment capture rate of catch basins under extended conditions and the results are shown in Figure 3.

As is indicated, the maximum flow rate in numerical simulations was extended to 84 L/s, which is about three times those in the experiments. Also, the numerical predictions compare well with the measurements when the particle size is larger than 0.25 mm. Larger flow rates result in lower capture rates due to the large flow velocity and strong turbulence intensity. Also, smaller sediments are more difficult to capture. For the largest particles (1.8 mm) in this study, nearly all the particles can be captured when the flow rate is smaller than 30 L/s, and the catch basin still has a capture rate of over 70% at a flow rate of 84 L/s. For particles with sizes from 0.25 to 0.4 mm, the capture rate is over 60% when flow rate is less than 30 L/s, and the capture rate decreases to around 40% when the flow rate is over 80 L/s. For particles of 0.1 mm, the predictions overestimate the capture efficiency by around 5–10%, and the degree of overestimation increases with the decrease in particle size: the predictions overestimate the capture efficiency

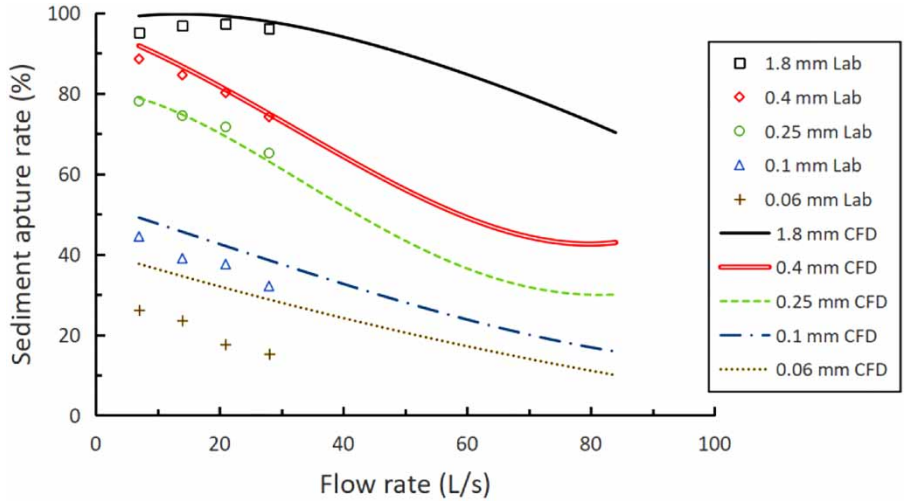

Figure 3 | CFD predicted sediment capture rate compared with the measurements of Tang *et al.* (2016) for different particle sizes.

by around 20% for particles of 0.06 mm. There are a number of reasons that possibly contribute this difference. One of which is that in the particle tracking simulation, the particle movement is calculated by the time-averaged flow velocity. For smaller particles, however, they can be resuspended by flow turbulence even with zero mean velocity. Additionally, the resuspension of the settled particles will also affect the capture efficiency. Further research is needed in modeling fine particles.

Previous studies (e.g. Avila *et al.* 2008; Howard *et al.* 2011; Tang *et al.* 2016) have concluded that flow rate, particle size, particle density and water depth are important factors affecting sediment capture rate in catch basins. The ability to gain insights into flow field and particle transport process makes the numerical simulation a good tool to help investigate the influence of these factors. In this study, the velocity fields in the catch basin under different flow rates were compared by contours and vectors in Figure 4.

In Figure 4, the contours show the distributions of the velocity magnitude, and the vectors indicate the local fluid velocity. At a larger flow rate, the water level is higher, also, the falling jets can plunge into a deeper area, consistent with the experimental measurements of Tang *et al.* (2016). Although scenarios with different flow rates show different water levels, the circulation patterns are similar. From the front views, there are two circulations located at both sides of the center line with nearly symmetrical distribution. The position of the circulation center is found not to be influenced by the flow rate, which is located at the level of around 0.25 m above the structure bottom. The larger flow rate results in faster circulation flow, for example, at the level of 0.25 m above the bottom (the level of circulation

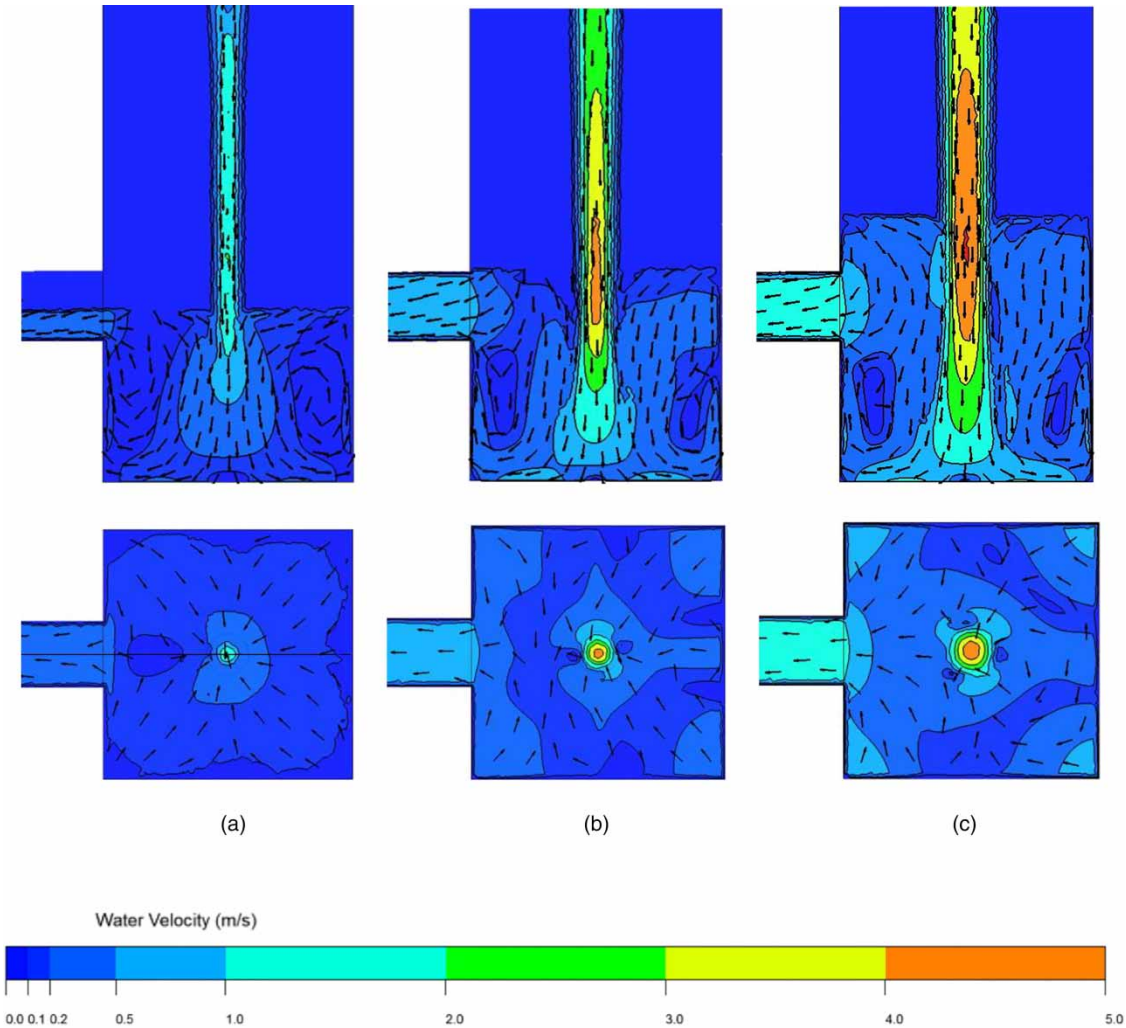

Figure 4 | Water velocity vectors of the front view (center section) and top view at a level of 0.1 m above the outlet pipe invert for a flow rate of: (a) 7 L/s; (b) 28 L/s; (c) 56 L/s.

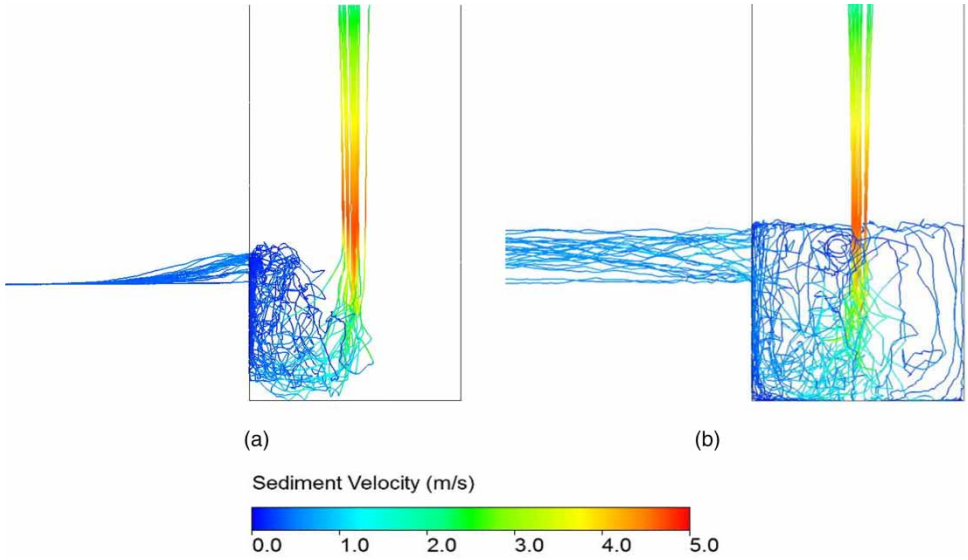

Figure 5 | Trajectories of the escaped particles in the catch basin at a flow rate of 28 L/s (a) for particles of 1.8 mm, (b) 0.1 mm. Please refer to the online version of this paper to see this figure in color: http://dx.doi.org/10.2166/wst.2018.009.

center). The maximum velocity in the circulation is 0.15 m/s at the flow rate of 7 L/s. This value increases to 0.4 m/s when the flow rate is 28 L/s and further to 0.6 m/s when the flow rate is 56 L/s. The top view shows the horizontal flow at the level of 0.1 m above the outlet pipe invert, and the velocity near the outlet area is greater due to the contraction of the boundary.

To understand how particles are influenced by the flow field, the trajectories of the escaped particles are plotted in Figure 5, where colors represent the magnitude of the velocity. The particles are carried by the inflow and their velocities rise while falling through the air. After the particles fall into the sump, there is a rapid velocity decrease mainly due to the slowdown of the water jet velocity. In the sump, the particles can be carried upwards by the circulation and then carried out by the flow pointing to the outlet. The escaped particles are more likely to appear on the left side compared to the right side due to the effect of the outlet. The settling process versus the escape process determines the final capture rates.

Validated numerical models can be used to investigate the influence of different structural designs. To investigate the influence of the sump, the conditions with and without a sump in the catch basin were compared. In addition, without changing the sump structure and the inflow rate, the influence of inflow arrangement was also studied, and the scenarios with inflow coming into the sump horizontally instead of vertically were simulated. The results are shown in Figure 6.

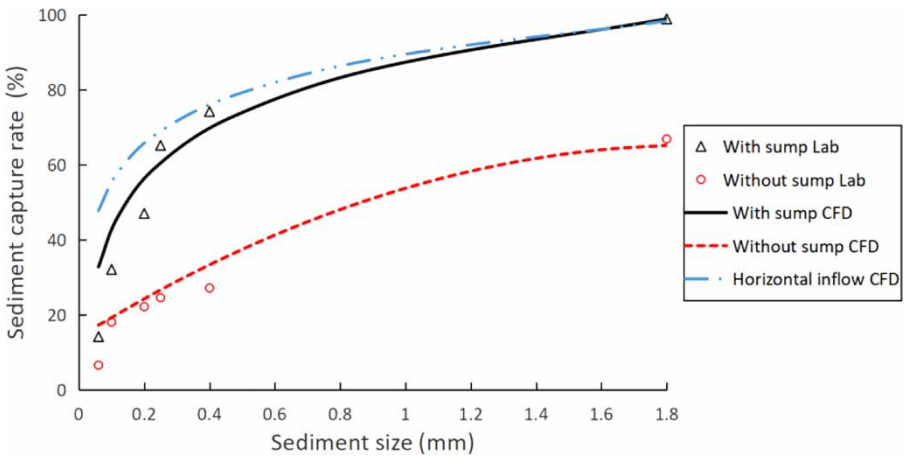

Figure 6 | Sediment capture rates in different catch basin structures at a flow rate of 28 L/s.

From Figure 6, when the particle is small, the simulations similarly overestimate the capture rate with and without the sump. The sump is shown to play an important role in improving sediment capture as the capture rate is increased by 20% compared to that without the sump. This difference decreases when particles are smaller than 0.2 mm. When the inflow direction is changed to horizontal, the flow field in the sump changes. According to the simulated streamlines, the flow moves forward in a spiral way in the sump, which leads to a longer traveling distance and an increased rate of around 10%.

Previous studies (e.g. Avila *et al.* 2008; Howard *et al.* 2011; Tang *et al.* 2016) proposed some equations based on the Péclet number P, which is the ratio of settling velocity to the mean flow velocity. However, the horizontal mean flow velocity requires knowledge of the water depth. In this study, P is calculated by dividing the vertical mean flow velocity by the sediment settling velocity. The settling velocity V_s is always regarded as the key variable to determine the settling ability as it integrates the effect of several important factors including particle density and particle size. A number of methods can be used to calculate the settling velocity (Gu *et al.* 2016). In this study, it is estimated using the equation suggested by Ferguson & Church (2004):

$$\mathrm{V_s} = \frac{((\rho_p - \rho_w)gd_p^2)/\rho_w}{C_1\nu + \left[0.75C_2(\rho_p - \rho_w)gd_p^3/\rho_w\right]^{0.5}} \tag{3}$$

where ν is kinematic viscosity and d_p is the particle size. Ferguson & Church (2004) suggested $C_1 = 18$ and $C_2 = 1.0$ for typical natural sands. In this study, the Péclet number P can be written as follows:

$$P = \frac{V_s}{(Q/\mathrm{A}_h)} \tag{4}$$

where A_h is the horizontal cross-sectional area, and Q is the inlet flow rate. The measured capture rates (Tang *et al.* 2016) and the measurements in other scenarios (Howard *et al.* 2011; Ma & Zhu 2014) are then expressed as a function

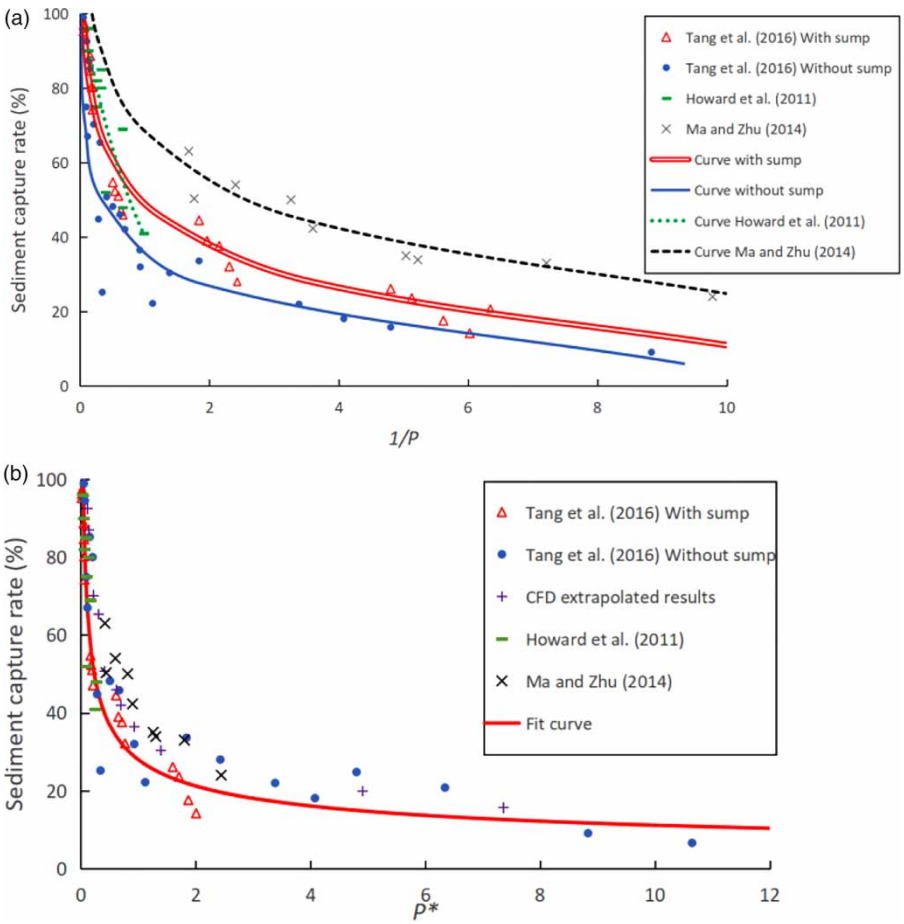

Figure 7 | Sediment capture rate (a) as a function of 1/*P*, (b) as a function of *P**.

of $1/P$, and the results are shown in Figure 7(a). As is shown, in each scenario a strong correlation can be found between the sediment capture rate and $1/P$, and they can be expressed as several curves. However, these curves have distinct curvatures because their sump depths are different. Therefore, to obtain a more general relationship, a dimensionless parameter P^* is then defined by incorporating the sump depth:

$$P^* = \frac{D_{out}}{P(H' + D_{out})} \tag{5}$$

where H' is the depth of the sump and the D_{out} is the diameter of the outlet pipe. P^* includes the influence of the particle size, the particle density, the flow rate, the sump depth and the size of the catch basin. The previous measured results and the CFD extrapolated results are then expressed as a function of P^*, and the results are shown in Figure 7(b).

Figure 7 shows that the sediment capture rates from the CFD results as well as previous measurements (Howard *et al.* 2011; Ma & Zhu 2014; Tang *et al.* 2016) can be fitted nicely into an equation with P^*:

$$\eta_s = aP^{*-b} \tag{6}$$

where η_s is the capture rate, and the values for a and b are fitted using the data sets in Figure 7(b) as 0.28 and 0.4, respectively. In this study, particles with a large size of 1.8 mm are always in the far left of curve with $P^* < 0.2$, and particles with a small size of 0.06 mm are always in the right end of the curve with $P^* > 1.5$. This curve can also give reasonable predictions compared to the measurements in other structures.

CONCLUSIONS

In this study, a three-dimensional three-phase (air-water-solid) computational simulation using the Eulerian-Lagrangian tracking method was carried out with RNG k-ε turbulence closure model. Previous laboratory measurements (Tang *et al.* 2016) of water depth and sediment capture rates were used to validate the numerical results, and water velocity measurements (Howard *et al.* 2011) were used to validate the computed flow field. Under the same conditions, the CFD simulated results provide good agreement compared to the experimental results (Tang *et al.* 2016), but the simulations tend to overestimate the sediment capture ability when particles are smaller than 0.2 mm. Capture rates under larger water flow rates were tested. Under the maximum flow rate (84 L/s), the catch basin with the sump depth of 0.5 m still has a capture rate of 40% to 70% for particles larger than 0.25 mm. However, the catch basin with this sump depth is not very effective in capturing particles smaller than 0.1 mm. Also, various catch basin designs were compared and the existence of a sump structure improves the capture rate significantly by around 20% to 40%, while adjusting the inflow direction from vertical to horizontal is found to increase the capture rate by about 10%. With the help of numerical modeling, the flow field and the particle transport process were discussed, and an equation was developed to predict the capture rate in various scenarios.

REFERENCES

Almedeij, J., Ahmad, E. & Alhumoud, J. 2010 Representative particle size of sediment in storm sewer inlets. *American Journal of Environmental Sciences* **6** (4), 316.

ANSYS CFX 2013 Theory Guide ANSYS Inc.

Aronson, G., Watson, D. & Pisano, W. 1983 *Evaluation of Catch Basin Performance for Urban Stormwater Pollution Control. US EPA. Grant No. R-804578. EPA-600/ 2-83-043.* Cincinnati, OH, USA.

Avila, H., Pitt, R. & Durrans, S. R. 2008 Factors affecting scour of previously captured sediment from stormwater catch basin sumps. In: *Stormwater and Urban Water Systems Modeling, Monograph 16*, CHI, Guelph, Ontario.

Azimi, A. H., Zhu, D. Z. & Rajaratnam, N. 2012 Computational investigation of vertical slurry jets in water. *International Journal of Multiphase Flow* **47** (1), 94–114.

Bong, C., Lau, T. & Ghani, A. 2014 Sediment size and deposition characteristics in Malaysian urban concrete drains-a case study of Kuching city. *Urban Water Journal* **11** (1), 74–89.

Butler, D., Thedchanamoorthy, S. & Payne, J. A. 1992 Aspects of surface sediment characteristics on an urban catchment in London. *Water Science & Technology.* **25** (8), 13–19.

Chebbo, G., Musquere, P. & Bachoc, A. 1990 Solids transferred into sewers. In: *Proceedings of the 5th International Conference on Urban Storm Drainage*, Osaka, Japan.

Chrigui, M. 2005 *Eulerian-Lagrangian Approach for Modeling and Simulations of Turbulent Reactive Multi-Phase Flows Under gas Turbine Combustor Conditions*. PhD thesis, Technische Universitat Darmstadt.

City of Calgary 2011 *Stormwater Management and Design Manual*. The City of Calgary, Alberta, Canada. Available from: http://www.calgary.ca/PDA/pd/Documents/urban_development/bulletins/2011-stormwater-management-and-Design.pdf.

Clegg, S., Forster, C. F. & Crabtree, R. W. 1992 Sewer sediment characteristics and their variation with time. *Environmental Technology* **13** (6), 561–569.

Faram, M. G. & Harwood, R. 2000 The role of CFD as a tool for the development of wastewater treatment systems. In: *Fluent Users' Seminar*, 21–22 September, Sheffield, UK.

Faram, M. G. & Harwood, R. 2002 Assessment of the Effectiveness of Storm water Treatment Chambers Using Computational Fluid Dynamics. In: *9ICUD Conference*, Portland, Oregon, USA.

Ferguson, R. I. & Church, M. 2004 A simple universal equation for grain settling velocity. *Journal of Sedimentary Research* **74** (6), 933–937.

Fluent Manual 2005 *Manual and User Guide of Fluent Software*. Fluent Inc.

Gu, L., Dai, B., Zhu, D. Z., Hua, Z. L., Liu, X. D., van Duin, B. & Mahmood, K. 2016 Sediment modelling and design optimization for stormwater ponds. *Canadian Water Resources Journal* **42** (1), 70–87.

Howard, A. K., Mohseni, O., Gulliver, J. S. & Stefan, H. G. 2011 Hydraulic analysis of suspended sediment removal from storm water in a standard sump. *Journal of Hydraulic Engineering* **138** (6), 491–502.

Howard, A., Mohseni, O., Gulliver, J. S. & Stefan, H. G. 2012 Use of standard sumps for suspended sediment removal from stormwater. *Journal of Hydraulic Engineering* **138** (6), 491–502.

Kee, N. C. S. & Tan, R. B. H. 2002 CFD simulation of solids suspension in mixing vessels. *Canadian Journal of Chemical Engineering* **80** (4), 1–6.

Lager, J., Smith, W. G. & Tchobanoglous, G. 1977 *Catchbasin Technology Overview and Assessment. US EPA. EPA-600/2-77-051*. California, USA.

Ma, Y. & Zhu, D. Z. 2014 Improving sediment removal in standard stormwater sumps. *Water Science & Technology* **69** (10), 2099–2105.

Mohsin, M. & Kaushal, D. R. 2016 3D CFD validation of invert trap efficiency for sewer solid management using VOF model. *Water Science and Engineering* **9** (2), 106–114.

Niño, Y. & García, M. H. 1998 Using Lagrangian particle saltation observations for bedload sediment transport modelling. *Hydrological Processes* **12** (8), 1197–1218.

Sha, Z., Oinas, P., Louhi-Kultanen, M., Yang, G. & Palosaari, S. 2001 Application of CFD simulation to suspension crystallization factors affecting size-dependent classification. *Powder Technology* **121** (1), 20–25.

Tang, Y. B., Zhu, D. Z., Rajaratnam, N. & van Duin, B. 2016 Experimental study of hydraulics and sediment capture efficiency in catch basins. *Water Science & Technology* **74** (11), 2717–2726.

Thinglas, T. & Kaushal, D. R. 2008 Comparison of two and three dimensional modeling of invert trap for sewer solid management. *Particuology* **6** (3), 176–184.

Virdung, T. & Rasmuson, A. 2007 Hydrodynamic properties of a turbulent confined solid-liquid jet evaluated using PIV and CFD. *Chemical Engineering Science* **62** (21), 5963–5979.

Wang, F., Mao, Z., Wang, Y. & Yang, C. 2006 Measurement of phase holdups in liquid-liquid-solid three-phase stirred tanks and CFD simulation. *Chemical Engineering Science* **61** (20), 7535–7550.

Wilson, M. A., Mohseni, O. M., Gulliver, J., Hozalski, R. M. & Stefan, H. G. 2009 Assessment of hydrodynamic separators for storm-water treatment. *Journal of Hydraulic Engineering* **135** (5), 383–392.

Wörner, M. 2003 A Compact Introduction to the Numerical Modeling of Multiphase Flows. In: *Wissenschaftliche berichte FZKA 6932. Forschungszentrum Karlsruhe in der Helmholtz-Gemeinschaft*, Karlsruhe, Germany.

First received 20 July 2017; accepted in revised form 6 November 2017. Available online 11 January 2018